Published in final edited form as:
Nat Neurosci. 2009 June ; 12(6): 801–807. doi:10.1038/nn.2305.

COHERENT GAMMA OSCILLATIONS COUPLE THE AMYGDALA AND STRIATUM DURING LEARNING

Andrei T. Popescu, **Daniela Popa**, and **Denis Paré**
Center for Molecular & Behavioral Neuroscience, Rutgers State University, 197 University Ave., Newark, NJ 07102

Abstract

The basolateral amygdala (BLA) mediates the facilitating effects of emotions on memory. The BLA enhancing influence extends to various types of memories, including striatal–dependent habit formation. To shed light on the underlying mechanisms, we performed unit and local field potentials (LFP) recordings in BLA, striatum, auditory cortex, and intralaminar thalamus in cats trained on a stimulus-response task where the presentation of one of two tones (CS+) predicted reward delivery. The coherence of BLA but not cortical or thalamic LFPs was highest with striatal gamma activity and intra-BLA muscimol infusions selectively reduced striatal gamma power. Moreover, coupling of BLA-striatal unit activity increased when LFP gamma power augmented. Early in training, the CS+ and unrewarded tone elicited a modest increase in coherent BLA-striatal gamma. As learning progressed, this gamma coupling selectively increased in relation to the CS+. Thus, coherent gamma oscillations coordinate amygdalostriatal interactions during learning and might facilitate synaptic plasticity.

Emotional arousal generally enhances memory[1] and much data suggest that the basolateral amygdala (BLA) is responsible for this effect[2]. Emotionally arousing events and their anticipation cause increases in the firing rate of BLA neurons[3,4]. Pharmacological interventions that interfere with this enhanced BLA activity decrease memory for events that took place shortly before, in many learning tasks[5]. On the inhibitory avoidance task for instance, intra-BLA infusions of GABA agonists[6], or glutamate receptor antagonists[7] just after training reduce longterm recall measured days later, well after the effects of these drugs have dissipated. Conversely, drugs that presumably enhance BLA activity such as bicuculline[8], as well as agonists of beta-adrenergic[9] and muscarinic[10] receptors enhance recall when injected within two hours after training, but not later.

In contrast with Pavlovian cued fear learning[11,12], the above effects do not depend on storage in the BLA but in other structures that receive BLA inputs. For instance, post-learning intra-BLA infusion of amphetamine increases striatal-dependent storage of response information and hippocampal-dependent storage of spatial information. In contrast, infusing lidocaine in the BLA shortly before testing long-term recall has no effect on either task[13]. Overall, these findings imply that during emotional arousal, the BLA facilitates memory consolidation in other brain structures. This effect extends to various types of memories, including types of motor learning that depend on striatal plasticity.

Correspondence should be sent to: Denis Paré, Center for Molecular & Behavioral Neuroscience, Rutgers, The State University of New Jersey, 197 University Avenue, Newark, NJ 07102, Phone: (973) 353-1080 ext 3251, Fax: (973) 3531255, Email: pare@axon.rutgers.edu.

Competing interests statement
The authors declare that they have no competing financial interests.

Consistent with this, we have shown that BLA inputs can facilitate induction of corticostriatal long-term potentiation[14]. However, because these experiments involved the delivery of electrical stimuli *in vitro*, how the amygdala and striatum interact during learning *in vivo* remains unclear. Here, we addressed this question by performing extracellular recordings of unit activity and local field potentials (LFPs) in basal amygdaloid nuclei, striatum, auditory cortex, and intralaminar thalamic nuclei during the acquisition of a stimulus-response task known to depend on striatal plasticity[15].

RESULTS

Database

Unit activity and LFPs were recorded in six cats using high-impedance tungsten microelectrodes. All striatal recordings were obtained in a ventral sector of the putamen adjacent to the amygdala, where neostriatal projections of the cat BLA are densest[16]. Histological controls (Supplementary Fig. 1) revealed that our sample of extracellularly recorded cells included 139 striatal, 159 cortical, 55 thalamic intralaminar, and 152 BLA neurons. Analyses of firing rates and spike durations (Supplementary Fig. 2) revealed that within each structure, ≥ 70% of the neurons fell in one dominant cell class. These neurons presumably correspond to principal striatal (medium spiny), cortical (pyramidal or stellate), thalamic (relay), or BLA (pyramidal) neurons. The following analyses are restricted to these dominant classes of neurons.

Correlated amygdalo-striatal activity in the waking state

In search of a possible physiological signature of amygdalostriatal interactions, we first analyzed the coherence spectra of simultaneously recorded BLA and striatal LFPs during epochs of spontaneous waking (Fig. 1a). This analysis revealed that except for frequencies below 3 Hz, coherence of BLA and striatal LFPs was maximal in the gamma range (35–45 Hz). To test if this property also applied to other major striatal inputs, we carried out the same analysis between striatal and cortical (Fig. 1b) or between striatal and thalamic (Fig. 1c) LFPs. Whereas all combinations of recording sites showed coherent low frequency activity, the coherence of gamma oscillations was much higher between striatal and BLA LFPs ($F(2,3819) = 1255.64$, $p < 0.0001$). In contrast, the coherence of BLA and thalamic or cortical gamma was low (Supplementary Fig. 3).

Importantly, the same weak relationship was seen between striatal gamma vs. cortical or thalamic gamma whether we separately considered primary or associative auditory areas as well as posterior or anterior intralaminar thalamic nuclei. For instance, Figure 1d shows digitally filtered LFPs (35–45 Hz) for two cortical (primary, top; associative, bottom), thalamic (anterior, top; posterior, bottom) striatal, and BLA sites. Visual inspection of these signals confirmed the preferential coupling of striatal gamma to BLA activity, relative to thalamic and cortical fast oscillations. One possible explanation for this result could be that BLA recording sites are physically closer to the striatum than thalamic or cortical recording sites. At odds with this possibility however, the same results were obtained when we separately considered BLA, cortical, and thalamic recording sites that were equidistant from the striatum (Supplementary Fig. 4).

Next, we obtained quantitative estimates of the phase relationship between striatal gamma vs. cortical, thalamic, or BLA gamma (Fig. 1e–h). To this end, striatal gamma cycles of high amplitude (≥ 2.5 SD of average) were identified and the interval between the peak of the striatal gamma cycles vs. the other sites was measured. Figure 1i–k plots these phase lags (x-axis) against the amplitude of the corresponding gamma cycles (left y-axis), normalized to the amplitude of striatal gamma. Although average phase lags were similar at all recording sites,

they were much more variable at cortical (Fig. 1i) and thalamic (Fig. 1j) sites than in the BLA (Fig. 1k). The significance of this difference was assessed by computing an ANOVA on the cycle-to-cycle deviations from the average phase lag for the three combinations of recording sites ($F(2,7317) = 1526.5$, $p < 0.0001$). A similarly variable phase relationship was seen between BLA and cortical or thalamic gamma (Supplementary Fig. 5). There was an average 40 ± 14 degrees phase shift between BLA and striatal gamma. We observed no relationship between the distance separating the BLA and striatal recording sites and phase lags ($r = 0.001$; Supplementary Fig. 6).

To determine whether the coherent gamma activity seen in the BLA and striatum resulted from the influence of a common input or if the BLA contributed to generate gamma activity in the striatum, we compared the effects of bilateral intra-BLA infusions of the same volume (1 μl/hemisphere) of saline (n = 4) or muscimol (n = 5; 4 μM in saline) on striatal LFP power. Here, it should be noted that the volume of the cat BLA is much higher than in rats, the cat basolateral nucleus spanning > 4 mm in the dorsoventral axis, compared to 1 mm in rats. Thus, to expose as many BLA neurons to muscimol as possible while minimizing mechanical distortion of the tissue and muscimol diffusion outside BLA, the total injected volume (1 μl/hemisphere) was divided in ten 0.1 μl infusion sites separated by 0.2 mm along a single dorsoventral microsyringe track that spanned the central 2 mm of the BLA. In each subject, this process was repeated sequentially in both hemispheres, resulting in total infusion times of 25 minutes. Whereas intra-BLA saline infusions had no effect on striatal LFP activity (Fig. 2a,d; black trace in Fig. 2c; post-hoc paired *t*-test, $P = 0.2$), muscimol infusions caused a statistically significant reduction of striatal LFP power that was mostly restricted to gamma activity (Fig. 2b,c, red lines; paired *t*-test, $P = 0.0005$; Supplementary figure 7).

To examine the relationship between gamma oscillations and unit activity in the BLA and striatum, we constructed peri-event histograms (PEHs) of unit activity around the positive peaks of gamma oscillations recorded by the same microelectrode as the unit activity. To this end, we first isolated gamma by digitally filtering the LFPs and then identified gamma cycles with positive peak exceeding the average plus 2.5 SD of the filtered signal (Fig. 3a). Then, we computed histograms of firing for each cell around these reference times. Figure 3 shows examples of such PEHs for BLA (Fig. 3b), and striatal neurons (Fig. 3c). Although the PEHs of figure 3b–c give the impression that BLA and striatal cells fired repetitively in relation to gamma, this was not usually the case. In fact, although gamma activity typically occurred in short bursts comprised of 2–6 consecutive high amplitude cycles, BLA and striatal cells fired infrequently during each burst (BLA 0.16 ± 0.02 spikes/burst; striatum, 0.18 ± 0.04 spikes/bursts).

To determine whether the gamma modulations of unit activity seen in the PEHs were statistically significant, we computed a rhythmicity index (RI) for each cell. The RI was obtained by averaging the difference in spike counts between the three center peaks and troughs of the PEHs and dividing the result by the average of the entire histogram to normalize for variations in firing rates. Statistical significance of the RI was tested by recomputing the peri-event histograms after shuffling the spike times, repeating this process 1000 times. The actual RI was considered significant if it was higher than 95% of the randomly-generated RIs. Using this approach, it was determined that the activity of 49% of BLA and 28% of striatal cells was significantly modulated by gamma activity. Next, we examined when BLA and striatal cells fired with respect to gamma activity. To this end, for each cell with a significant RI, we located the bin with the highest counts in the PEHs and computed a frequency distribution of peak times. As shown in Fig. 3d–e, this revealed a similar entrainment of BLA and striatal unit activity by local gamma with both cell types firing preferentially during the rising phase of positive gamma cycles. The same relation was found for thalamic and cortical units (Supplementary Fig. 8).

To test whether gamma activity affected functional coupling between BLA and striatal neurons, we examined how LFP power in different frequency bands affected the correlation between striatal and BLA unit activity. To this end, we first crosscorrelated unit activity in 362 couples of simultaneously recorded BLA and striatal neurons. With rare exceptions, these crosscorrelograms were flat (Fig. 3f). However, when we excluded striatal spikes occurring during periods of low (< 2.5SD) gamma power, many crosscorrelograms exhibited significant coupling (Fig. 3g). Significance of the correlograms was assessed by shuffling each of the BLA spike trains 1000 times, recomputing the correlogram each time, and comparing the actual correlogram to the randomly-generated values. A correlogram was considered significant when the sum of its central bins (± 5ms from origin) was higher than that in 95% of the randomly-generated correlograms. To quantify how the incidence of significant BLA-striatal correlations changed in relation to gamma activity, each cell couple was assigned a correlation index (by comparing the sum of the central ± 5 ms bins of the correlograms to that of the randomly-generated correlograms). The correlation indexes were then rank ordered from the lowest (left) to the highest (right) and expressed as percentiles (Fig. 3h). Figure 3h shows the frequency distribution of these correlations indexes for the correlograms including all spikes vs. those computed during periods of high amplitude striatal gamma. The proportion of correlograms with central bins ≥ 2.5 SD was 15% during high amplitude gamma, compared to 8% when all spikes were considered. To determine whether this was statistically significant, we performed a X^2-test analysis comparing the incidence of cell couples with central crosscorrelograms peaks higher vs. lower than 2.5 SD when all spikes were included vs. only those occurring during periods of high amplitude striatal gamma. The difference was significant ($P = 0.0042$).

To test whether this enhancement of BLA-striatal unit coupling was selective to gamma related activity, we repeated this analysis in various frequency bands by digitally filtering LFPs in sliding windows of 5 Hz. Using this approach, we observed that significant increases in BLA-unit coupling preferentially occurred in relation to gamma activity (Fig. 3i). Moreover, when the same analysis was repeated for all available couples of simultaneously recorded cortical and striatal cells (n = 298; Fig. 3j), or thalamic and striatal (n = 82; Fig. 3k) neurons, this enhancement of unit correlations by gamma activity was found to be selective to BLA-striatal activity (X^2-tests: corticostriatal, $P = 0.88$; thalamostriatal, $P = 0.29$). Carrying out the same analysis for cortical and BLA or thalamic and BLA cell couples failed to reveal a facilitation of unit coupling by gamma activity (Supplementary figure 9).

To determine whether the increased BLA-striatal coupling revealed above was due to increased discharge rates, we compared baseline firing rates to those seen during periods of high gamma power (> 2.5 SD). However, increases in gamma power were not associated with changes in the firing rates of BLA (% change from low to high gamma of 3.2 ± 8.7%; paired *t*-test, $P = 0.14$) or striatal (14.4 ± 19.6 %; paired *t*-test, $P = 0.41$) neurons.

Overall, the above suggests that BLA neurons impose gamma activity to the striatum and that functional coupling between BLA and striatal cells is highest during periods of high amplitude gamma. Thus, coherent striatal and BLA gamma LFP activity is a physiological signature of amygdalo-striatal interactions. Importantly, this increased coupling of BLA and striatal activity by gamma is not associated with changes in firing rates.

Coordination of amygdalostriatal interactions by gamma during learning

To investigate whether gamma oscillations also coordinate amygdalostriatal interactions during learning, cats were trained on a stimulus-response task. Memory formation on such tasks is striatal-dependent (reviewed in[15]). In our case (Fig. 4a), cats that had restricted access to food gradually learned that the termination of one of two tones (CS+, 3 sec) coincided with the brief availability (1 sec) of a liquid food reward.

Each daily training session, the cats received around 60 randomly-interspersed presentations of the CS+ and CS− with variable inter-trial intervals (range 20–40 sec). Five consecutive daily training sessions occurred with the same CS+ prior to switching reinforcement contingencies. Learning progression was assessed by measuring the rate of anticipatory licking during the CS +, prior to reward delivery.

Figure 4b illustrates licking rate (y-axis) around the CS+ (black) and CS− (red) during trials obtained during the first (dashed lines) and last (continuous lines) two training sessions (averaged across all cats). Although the rate of anticipatory licking during the two tones (shaded area) did not differ significantly at early stages of training (Sessions 1–2, $F(1,1431) = 0.252$, $P = 0.615$), the difference became significant at late training stages (Sessions 4–5, $F(1,967) = 9.8$, $P = 0.0018$). Plotting the proportion of CS+ and CS− trials with anticipatory licking as a function of daily training sessions (Fig. 4c) revealed that the difference between the CS+, CS − and spontaneous licking reached statistical significance at the third training session ($F(2,890) = 11.6$, $P < 0.0001$).

Previous studies using stimulus-response tasks have revealed that BLA unit activity encodes expected outcomes[17–20]. In support of the idea that this information is used during learning, it was reported that BLA-lesioned animals are impaired at associating reward values to specific stimuli in a similar stimulus-response task[21]. Moreover, it was shown that BLA is required for cue-evoked excitation of nucleus accumbens neurons[22]. These results suggest that BLA might bring an emotional or motivational component to striatal processing during learning.

Consistent with this, we observed a strong parallel between improvements in behavioral performance and correlated amygdalostriatal gamma during the acquisition of this task (Fig. 5; $F(1,10) = 6.072$, $P = 0.0334$). Early in training (Fig. 5a,b), when the rates of anticipatory licking during the two tones were statistically indistinguishable, the CS+ (black) and unrewarded tone (red) elicited a modest but significant increase in coherent BLA-striatal gamma (paired *t*-test, $P = 0.005$). However, at this initial stage of training, the increase in coherent BLA-striatal gamma elicited by the two tones were statistically indistinguishable (paired *t*-test, days 1–2, $P = 0.72$). As learning progressed, the CS-related BLA-striatal gamma coupling augmented and became significantly more important in response to the CS+ (Fig. 5c–e; paired *t*-test, days 1–2 vs. days 3–5, $P = 0.002$; *t*-test, CS+ vs. CS− on days 3–5, $P = 0.0001$). Importantly, the first training session where the CS+ elicited significantly larger increases in coherent amygdalostriatal gamma activity than the CS− (Fig. 5c, Day 3) coincided with the training session where behavioral evidence of discrimination between the CS+ and CS− became maximal (Fig. 4c, Day 3). Moreover, when the reinforcement contingencies were reversed (Fig. 5f–h), the identity of the CS eliciting larger increases in coherent BLA-striatal gamma switched and the time course of this effect again paralleled the evolution of behavioral improvements (compare Fig. 5i and Fig. 4c).

Further supporting the notion that increases in coherent BLA-striatal gamma are closely related to learning on this task, a significant positive correlation was found between the proportion of trials with anticipatory licking in a given session vs. the difference in coherent BLA-striatal gamma elicited by the two tones in the same session ($r = 0.55$, $P < 0.01$; Fig. 6a). Yet, the increase in coherent BLA-striatal gamma was not a simple motor correlate since trials with vs. without anticipatory licking did not differ in this respect (Fig. 6b). Importantly, learning-related changes in correlated gamma were only seen between BLA and striatal recording sites, not between striatal and cortical or striatal and thalamic sites (Supplementary Fig. 10a–c). Moreover, examination of learning related fluctuations in other frequency bands shown in Fig. 3j,k to increase coupling between striatal and cortical or thalamic units failed to reveal significant changes (Supplementary Fig. 10d,e).

DISCUSSION

The present study was undertaken to shed light on amygdalo-striatal interactions during memory formation. The interest of this question stems from pharmaco-behavioral studies implicating BLA activity in the facilitation of striatal-dependent memories by emotional arousal. Our results indicate that gamma oscillations originating in the BLA coordinate amygdalo-striatal interactions. Indeed, not only were BLA and striatal LFPs most coherent in the gamma range, but these fast oscillations greatly facilitated coupling of BLA and striatal firing, more so than oscillations in other frequency bands. Moreover, during the acquisition of a striatal-dependent stimulus-response task, the coherence of CS-evoked BLA-striatal gamma increased in parallel with improvements in behavioral performance.

Striatal contributions to memory

Beginning in the 1960s, several studies showed that striatal lesions interfere with the acquisition of various learning tasks (reviewed in[15,23,24]). However, because such lesions might have impaired non-mnemonic functions, it remained unclear whether the striatum participated in memory formation. Evidence in support of this role came from studies where striatal activity was manipulated right after training by performing local drug infusions. For instance, long-term striatal dependent memories can be enhanced by immediate post-training injections of amphetamines as well as dopaminergic or muscarinic receptor agonists[25–29]. Moreover, intrastriatal infusions of the NMDA antagonists AP5 or MK-801 immediately after training on a striatal-dependent task interfere with memory[30,31], but not at longer delays. These observations strongly suggest that the striatum is not only required for performance but a critical site for memory formation and/or storage[23,24]).

Additional evidence for a role of the striatum in memory, independent of its contribution to motor control, came from lesion studies that used pairs of learning tasks sharing the same motivational, sensory, and motor features but where performance relies on different strategies and cerebral networks. In one study for instance[32], rats could learn the location of a submerged platform in a water maze by either remembering the location of the platform or of a cue indicating where the platform was located. Striatal lesions selectively interfered with performance in the cued-version of the task whereas fornix lesions interfered with its spatial version.

Facilitation of striatal memory formation by BLA activity

A large body of evidence indicates that BLA activity facilitates memory in a variety of learning tasks where memory formation depends on different networks[2]. In one study for instance[13], immediate post-training infusions of amphetamines locally in the BLA facilitated memory formation for the cued (striatal-dependent) and spatial (hippocampal-dependent) versions of the task. In contrast, infusing lidocaine in the BLA shortly before testing long-term recall had no effect on either task[13], indicating that the BLA is not the storage site of the facilitated memory but that it is involved transiently during and/or shortly after training to facilitate memory formation in the striatum and hippocampal formation.

In keeping with these observations, BLA activity was also shown to facilitate the induction of activity-dependent synaptic plasticity in a variety of structures, some of which are not directly connected to the BLA. For instance, BLA stimulation after LTP induction can enhance and stabilize LTP of perforant path inputs to the dentate gyrus[33–35] and thalamic inputs to the visual cortex[36].

How do BLA inputs facilitate memory formation and synaptic plasticity? The available evidence suggests that multiple parallel mechanisms are involved. One contributing factor

resides in the ability of the amygdala to recruit basal forebrain cholinergic neurons that project to the cerebral cortex, resulting in facilitated synaptic plasticity in cortical networks (reviewed in[37]). This would explain how BLA stimulation facilitates activity-dependent synaptic plasticity in structures, which in rodents and felines, are devoid of BLA inputs like the visual cortex[36] and dentate gyrus[33–35]. In support of this, it was reported that muscarinic receptor blockade interferes with the stabilizing and facilitating effects of BLA stimulation on LTP of thalamocortical[36] and perforant path[34] inputs. However, since the striatum receives little if any inputs from the basal forebrain[38], another mechanism must be involved.

Consistent with this, we reported that the NMDA-to-AMPA ratio is nearly twice as high at BLA compared to cortical synapses onto principal striatal neurons and that co-activation of BLA and cortical inputs greatly facilitates LTP induction at corticostriatal synapses[14]. Moreover, by selectively blocking NMDA receptors at BLA or cortical synapses onto principal striatal neurons, this same study showed that NMDA receptor activation at BLA inputs was required for the facilitation of corticostriatal LTP by BLA stimulation. However, the facilitation of corticostriatal synapses by BLA activity seen in this *in vitro* study required that BLA and cortical inputs coincide with firing of the postsynaptic cell, triggered by injection of large depolarizing currents. As a result, it remained unclear how natural activity patterns could bring about such levels of depolarization.

Coherent gamma oscillations as a physiological substrate of amygdalo-striatal interactions

The present study sheds light on this question by showing that BLA neurons generate periods of gamma activity in the striatum. Indeed, the fact the intra-BLA muscimol infusions caused a selective decrease in striatal gamma constitutes strong evidence that it was generated in the BLA, not by a common input to the BLA and striatum. Moreover, coupling between BLA and striatal unit activity was selectively increased during periods of high striatal gamma. The depolarization of medium spiny neurons produced by the arrival of BLA inputs at the gamma frequency probably contributes to enhance NMDA receptor activation and calcium influx in medium spiny neurons, thereby facilitating induction of heterosynaptic activity-dependent plasticity, as recently described *in vitro*[14].

Consistent with this, the present study also disclosed a close temporal relationship between coherent amygdalostriatal gamma and striatal-dependent learning. Indeed, the emergence of CS+-specific coherent amygdalostriatal gamma activity occurred during the same training session as when behavioral evidence of discrimination between the CS+ and unrewarded tones first reached significance. Importantly, evidence that gamma activity generated in the BLA contributes to the induction of learning-related synaptic plasticity was also obtained in other targets of the BLA. For instance, it was reported that during the acquisition of an appetitive trace-conditioning task, thought to be dependent on the hippocampus, the CS gradually acquired the ability to evoke coherent gamma oscillations in the BLA and rhinal cortices[39] and that this effect contributed to enhance rhinal transfer of neocortical inputs to the hippocampus[40,41]. Together with these earlier studies, our data suggest that the amygdale-mediated facilitation of memory depends on the ability the BLA to generate gamma oscillations that facilitate the induction of activity-dependent synaptic plasticity in target neurons.

METHODS

Surgery

Procedures were approved by the Institutional Animal Care and Use Committee of Rutgers State University, in compliance with the Guide for the Care and Use of Laboratory Animals (Department of Health and Human Services). Six adult male cats were pre-anesthetized with a mixture of ketamine and xylazine (15 and 2 mg/kg, i.m.) and artificially ventilated with a

mixture of ambient air, oxygen, and isoflurane. Atropine (0.05 mg/kg, i.m.) was administered to prevent secretions. The end-tidal CO_2 concentration was maintained at 3.7 ± 0.2 %, and the body temperature at 37–38°C using a heating pad. Bupivacaine (s.c.) was administered in the region to be incised 15 min prior to the first incision. In sterile conditions, an incision was performed on the midline of the scalp and the skull muscles were retracted. Then, a reference screw was inserted in the skull overlying the cerebellum and silver-ball electrodes were inserted in the supraorbital cavity to monitor eye movements. In addition, four screws were cemented to the skull to later fix the cat's head without pain or pressure. Finally, after trepanation and opening of the *dura mater*, an array of high-impedance tungsten microelectrodes (10–12 MΩ; Frederic Haer Co., Bowdoin, ME) was stereotaxically lowered to the regions of interest (see below).

Finally, the animals were administered penicillin (20,000 UI/kg, IM) and an analgesic (Ketophen, 2 mg/kg, s.c., daily for 3 days). Recording sessions began eight days after the surgery.

Recording sites and construction of microelectrode array

The microelectrode array included six electrodes aimed to the basal amygdala nuclei, eight electrodes aimed to the ventral striatum, eight electrodes aimed to primary or associative auditory cortical areas, and five electrodes aimed to rostral or posterior thalamic intralaminar nuclei. To construct the microelectrode array, a computer controlled milling machine was used to drill small holes in a Teflon block, at stereotaxically defined relative positions. Then, microelectrodes were inserted in the holes, adjusting the length of each microelectrode such that recordings could be obtained simultaneously from the various recording sites. After cementing the electrodes, the Teflon block was inserted in a tightly fitting Delrin sleeve, which was cemented to the skull. During the recording sessions, the electrodes could be lowered as a group by means of a micrometric screw.

Recordings

During the experiments, neuronal activity was sampled at ≥ 100 μm intervals. To insure mechanical stability, the microelectrodes were moved only once a day, 30 min prior to beginning data acquisition. The signals picked up by the electrodes (0.1 Hz-20 kHz) were observed on an oscilloscope, digitized, and stored on a hard disk. Spike sorting was performed off-line.

Muscimol injections

To assess the contribution of BLA activity to striatal gamma, we compared the effects of saline vs. muscimol infusions in the BLA on striatal gamma power. To this end, under isoflurane anesthesia and sterile conditions, two cats were implanted bilaterally with stainless steel guide cannulas aimed at the rostro-caudal center of the BLA, under stereotaxic guidance. The cannulas were positioned at the dorsal limit of the BLA, allowing full dorsoventral access for drug infusions. In these cats, we also placed tungsten microelectrodes in the striatum, as described above. After a one-week recovery from the surgery, the animals were gradually adapted to head restraint. During this period, they had restricted access to food, as for the subjects participating in the learning task (see below) and were only fed while in the recording room. Once adapted to head restraint, recording sessions began with a 15 min baseline recording period, after which a total volume of 1 μl/hemisphere of saline or muscimol (4 μM in saline) was infused in the BLA at a rate of 0.08μL/min. To this end, a microsyringe with a 25-gauge needle was lowered through the guide cannula and the solution was pressure-injected at ten equidistant sites (0.2 mm spacing) centered on the inner 2 mm of the BLA. The procedure was repeated for the contralateral side, and the recording continued for an additional 30 min. In both cats, two to three saline or muscimol infusions were performed on alternating days.

Behavior

Four cats that had restricted access to food (kept at 90% of their initial bodyweight) were trained on a stimulus-response task where the termination of one of two tones (CS+) coincided with the presentation of a liquid food reward (Gerber's pureed baby food "Sweet potatoes and turkey"; 2 ml/trial). The food was available for only 1 s, and the animals quickly learned to lick during this interval, consuming the food in more than 90% of CS+ presentations (even during the first training session). The CS+ and CS− tones lasted 3 sec and were presented in a random order with 20–40 s inter-tone intervals. The identity of the CS+ and CS− (3 or 12 kHz) was varied systematically across cats and had no effect on learning progression. Each daily training session, around 60 CS+ and 60 CS− trials were performed. Licking behavior was detected when the cats' tongues interrupted an infrared beam. The animals were only fed during the recording sessions. As a result, they were aroused and remained awake at all times (as assessed by EEG recordings). The cats' weight was monitored daily to maintain it within 10% of the initial value.

After five consecutive training sessions, the CS-reward contingencies were reversed. That is, the initial CS+ became CS−, and vice-versa. Three such reversal sessions (rD1-rD3 in Fig. 4–Fig. 5 and supplementary figure 10) were recorded.

Learning was assessed by monitoring the proportion of CS+ and CS− presentations during which anticipatory licking occurred. In addition, using the 3 sec windows preceding tone onsets, we computed the proportion of trials with spontaneous licking for comparison with tone-evoked behavior.

Histology

At the end of the experiments, recording sites were marked with electrolytic lesions (0.5 mA, 5–10 s). The animals were then given an overdose of sodium pentobarbital (50 mg/kg, i.v.) and perfused-fixed. The brains were later sectioned on a vibrating microtome (at 100 μm) and stained with cresyl violet to verify the position of recording electrodes. Microelectrode tracks were reconstructed by combining micrometer readings with the histology.

Data Analysis

Spike sorting—Data was analyzed offline with custom software written in Matlab 7.1 (The MathWorks Inc., Natick, MA). Spike-sorting was performed on digitally filtered data (high pass filter > 150 Hz), using principal component analysis and a supervised k-means clustering algorithm.

LFP analyses—To analyze LFP interactions in specific frequency bands, the raw data was filtered with a bandpass filter (width of 10 Hz), centered on the required frequency (e.g. results presented for 40 Hz correspond to data filtered in a 35–45 Hz band). For comparison purposes, all 2D and 3D histograms were normalized to the total number of events used, emphasizing their relative distribution rather than the absolute numbers.

Assessing the modulation of unit activity by gamma—To rule out the possibility that the gamma activity seen in the LFPs was volume conducted from a nearby structure, we computed peri-event histograms (PEHs) of unit activity around the peaks of positive gamma cycles ≥ the average plus 2.5 SD of the overall signal. In this case, the unit activity and LFPs were picked up by the same microelectrode. To eliminate the possibility that digital filtering at the gamma frequency introduced artefactual gamma activity, prior to filtering, the LFPs were down-sampled (from 1 point every 0.05 ms to 2 ms). This approach (as opposed to band-pass filtering the raw signal) abolishes most fast transients (like spikes) and greatly reduces the likelihood that spikes introduce artefactual gamma as a result of digital filtering. To determine

whether the gamma modulations of unit activity seen in the PEHs were statistically significant, we computed a rhythmicity index (RI) for each cell. The RI was obtained by averaging the difference in spike counts between the three center peaks and troughs of the PEHs and dividing the result by the average of the entire histogram to normalize for variations in firing rates. Statistical significance of the RI was tested by recomputing the peri-event histograms after shuffling the spike times, repeating this process 1000 times. The actual RI was considered significant if it was higher than 95% of the randomly-generated RIs.

Assessing gamma-related changes in unit coupling—The goal of these analyses is to test whether the occurrence of high amplitude gamma increased unit coupling in the BLA and striatum, as compared to when all spikes were crosscorrelated. To this end, for all BLA-striatal cell couples, we computed two crosscorrelograms of unit activity. The first included all spikes the cells generated. These correlograms were typically flat. The second kind of crosscorrelogram focused on periods when there was high amplitude gamma in the striatum. To compute these, we first searched striatal LFPs for periods of high amplitude gamma. Then, we crosscorrelated the unit activity taking place during these periods by ignoring all striatal spikes that did not coincide with high amplitude gamma (but including all BLA spikes). By comparing the two types of crosscorrelograms, one can assess whether unit coupling is altered during periods of high amplitude striatal gamma. We repeated this analysis for all cell couples. Each cell couple was assigned a correlation index (by comparing the sum of the central ± 5ms bins of the correlograms to that of the correlograms generated after shuffling of the BLA spike trains). The correlation indexes were then rank ordered from the lowest to the highest and expressed as percentiles. To test whether the gamma-related enhancement in BLA-striatal unit coupling where specific to gamma activity, the same analysis was repeated for all frequency bands (in bins of 5 Hz). Color-coded frequency distributions of the correlation indices were then plotted for all frequencies. Such distributions were typically characterized by a strong band at around −0.5 z-scores, corresponding to the median z-score. The median z-scores were not zero because the frequency distributions were skewed to the right. The cell couples with central peaks falling at the high end (right) of the distributions are those with significant correlations.

Learning-related fluctuations in gamma coherence—To study learning-related fluctuations in BLA-striatal coherence, power in the particular frequency band under consideration was calculated in one-second windows (sliding in 100 ms steps) around the onset of the two tones for the two recording sites. Coherence was estimated by computing the product of the powers for the two recoding sites for each one-second time window. Three factors must be taken into account when interpreting the results of these analyses. The first two relate to the physiology of the network under study. The third is methodological in nature. One factor is that from CS onset to the arrival of auditory impulses in the amygdala and striatum, is a short conduction delay, on the order of 20 ms in cats. A second factor is that before the increase in gamma coherence can be detected, BLA and striatal neurons must synchronize and this process necessarily requires a few gamma cycles. Third, reliable coherence measurements require that the epochs analyzed have a minimal duration to avoid spurious variability. By trial and error, we determined that a window duration of 1000 ms (sliding in steps of 100 ms) was the minimal duration to allow reliable coherence measurements while preserving an adequate temporal resolution. This means that the first data point during the CS includes the 500 ms immediately before the CS and the 500 ms after CS onset. This temporal smearing tends to reduce the amplitude of the initial CS-evoked changes in gamma coherence and cause a delay in its onset.

Statistical analyses—consisted of repeated measures ANOVAs followed by Bonferonni-corrected *t*-tests. All values are reported as average ± SEM.

Supplementary Material

Refer to Web version on PubMed Central for supplementary material.

Acknowledgements

This material is based upon work supported by NIMH grant RO1 MH073610 to Denis Paré.

REFERENCES

1. Christianson, SA. Hillsdale NJ: Erlbaum; 1992. Handbook of emotion and memory: current research and theory.
2. McGaugh JL. The amygdala modulates the consolidation of memories of emotionally arousing experiences. Annu Rev Neurosci 2004;27:1–28. [PubMed: 15217324]
3. Belova MA, Paton JJ, Morrison SE, Salzman CD. Expectation modulates neural responses to pleasant and aversive stimuli in primate amygdala. Neuron 2007;55:970–984. [PubMed: 17880899]
4. Pelletier JG, Likhtik E, Filali M, Pare D. Lasting increases in basolateral amygdala activity after emotional arousal: Implications for facilitated consolidation of emotional memories. Learn Mem 2005;12:96–102. [PubMed: 15805308]
5. Cahill L, McGaugh JL. Mechanisms of emotional arousal and lasting declarative memory. Trends Neurosci 1998;21:294–299. [PubMed: 9683321]
6. Castellano C, Brioni JD, Nagahara AH, McGaugh JL. Post-training systemic and intra-amygdala administration of the GABA-B agonist baclofen impairs retention. Behav Neural Biol 1989;52:170–179. [PubMed: 2552976]
7. Izquierdo I, et al. CNQX infused into rat hippocampus or amygdala disrupts the expression of memory of two different tasks. Behav Neural Biol 1993;59:1–4. [PubMed: 8095135]
8. Dickinson AH, Mesches MH, Coleman K, McGaugh JL. Bicuculline administered into the amygdala blocks benzodiazepine-induced amnesia. Behav Neural Biol 1993;60:1–4. [PubMed: 8216155]
9. Hatfield T, McGaugh JL. Norepinephrine infused into the basolateral amygdala posttraining enhances retention in a spatial water maze task. Neurobiol Learn Mem 1999;71:232–239. [PubMed: 10082642]
10. Salinas JA, Introini-Collison IB, Dalmaz C, McGaugh JL. Posttraining intraamygdala infusions of oxotremorine and propranolol modulate storage of memory for reductions in reward magnitude. Neurobiol Learn Mem 1997;68:51–59. [PubMed: 9195589]
11. LeDoux JE. Emotion circuits in the brain. Annu Rev Neurosci 2000;23:155–184. [PubMed: 10845062]
12. Pare D, Quirk GJ, Ledoux JE. New vistas on amygdala networks in conditioned fear. J Neurophysiol 2004;92:1–9. [PubMed: 15212433]
13. Packard MG, Cahill L, McGaugh JL. Amygdala modulation of hippocampal-dependent and caudate nucleus-dependent memory processes. Proc Natl Acad Sci U S A 1994;91:8477–8481. [PubMed: 8078906]
14. Popescu AT, Saghyan AA, Pare D. NMDA-dependent facilitation of corticostriatal plasticity by the amygdala. Proc Natl Acad Sci U S A 2007;104:341–346. [PubMed: 17182737]
15. Grahn JA, Parkinson JA, Owen AM. The cognitive functions of the caudate nucleus. Prog Neurobiol. 2008
16. Pare D, Smith Y, Pare JF. Intra-amygdaloid projections of the basolateral and basomedial nuclei in the cat: Phaseolus vulgaris-leucoagglutinin anterograde tracing at the light and electron microscopic level. Neuroscience 1995;69:567–583. [PubMed: 8552250]
17. Paton JJ, Belova MA, Morrison SE, Salzman CD. The primate amygdala represents the positive and negative value of visual stimuli during learning. Nature 2006;439:865–870. [PubMed: 16482160]
18. Saddoris MP, Gallagher M, Schoenbaum G. Rapid associative encoding in basolateral amygdala depends on connections with orbitofrontal cortex. Neuron 2005;46:321–331. [PubMed: 15848809]
19. Schoenbaum G, Chiba AA, Gallagher M. Orbitofrontal cortex and basolateral amygdala encode expected outcomes during learning. Nat Neurosci 1998;1:155–159. [PubMed: 10195132]

20. Schoenbaum G, Chiba AA, Gallagher M. Neural encoding in orbitofrontal cortex and basolateral amygdala during olfactory discrimination learning. J Neurosci 1999;19:1876–1884. [PubMed: 10024371]
21. Balleine BW, Killcross AS, Dickinson A. The effect of lesions of the basolateral amygdala on instrumental conditioning. J Neurosci 2003;23:666–675. [PubMed: 12533626]
22. Ambroggi F, Ishikawa A, Fields HL, Nicola SM. Basolateral amygdala neurons facilitate reward-seeking behavior by exciting nucleus accumbens neurons. Neuron 2008;59:648–661. [PubMed: 18760700]
23. Packard MG, Knowlton BJ. Learning and memory functions of the Basal Ganglia. Annu Rev Neurosci 2002;25:563–593. [PubMed: 12052921]
24. Yin HH, Knowlton BJ. The role of the basal ganglia in habit formation. Nat Rev Neurosci 2006;7:464–476. [PubMed: 16715055]
25. Carr GD, White NM. The relationship between stereotypy and memory improvement produced by amphetamine. Psychopharmacology (Berl) 1984;82:203–209. [PubMed: 6425900]
26. Packard MG, Teather LA. Posttraining estradiol injections enhance memory in ovariectomized rats: cholinergic blockade and synergism. Neurobiol Learn Mem 1997;68:172–188. [PubMed: 9322259]
27. Packard MG, Teather LA. Amygdala modulation of multiple memory systems: hippocampus and caudate-putamen. Neurobiol Learn Mem 1998;69:163–203. [PubMed: 9619995]
28. Packard MG, White NM. Dissociation of hippocampus and caudate nucleus memory systems by posttraining intracerebral injection of dopamine agonists. Behav Neurosci 1991;105:295–306. [PubMed: 1675062]
29. Viaud MD, White NM. Dissociation of visual and olfactory conditioning in the neostriatum of rats. Behav Brain Res 1989;32:31–42. [PubMed: 2930632]
30. Packard MG, Teather LA. Double dissociation of hippocampal and dorsal-striatal memory systems by posttraining intracerebral injections of 2-amino-5phosphonopentanoic acid. Behav Neurosci 1997;111:543–551. [PubMed: 9189269]
31. Packard MG, Teather LA. Posttraining injections of MK-801 produce a time-dependent impairment of memory in two water maze tasks. Neurobiol Learn Mem 1997;68:42–50. [PubMed: 9195588]
32. Packard MG, McGaugh JL. Double dissociation of fornix and caudate nucleus lesions on acquisition of two water maze tasks: further evidence for multiple memory systems. Behav Neurosci 1992;106:439–446. [PubMed: 1616610]
33. Akirav I, Richter-Levin G. Biphasic modulation of hippocampal plasticity by behavioral stress and basolateral amygdala stimulation in the rat. J Neurosci 1999;19:10530–10535. [PubMed: 10575049]
34. Frey S, Bergado-Rosado J, Seidenbecher T, Pape HC, Frey JU. Reinforcement of early long-term potentiation (early-LTP) in dentate gyrus by stimulation of the basolateral amygdala: Heterosynaptic induction mechanisms of late-LTP. J Neurosci 2001;21:3697–3703. [PubMed: 11331399]
35. Ikegaya Y, Saito H, Abe K. High-frequency stimulation of the basolateral amygdala facilitates the induction of long-term potentiation in the dentate gyrus in vivo. Neurosci Res 1995;22:203–207. [PubMed: 7566701]
36. Dringenberg HC, Kuo MC, Tomaszek S. Stabilization of thalamo-cortical long-term potentiation by the amygdala: cholinergic and transcription-dependent mechanisms. Eur J Neurosci 2004;20:557–565. [PubMed: 15233765]
37. Weinberger NM. Specific long-term memory traces in primary auditory cortex. Nat Rev Neurosci 2004;5:279–290. [PubMed: 15034553]
38. Mesulam MM, Mash D, Hersh L, Bothwell M, Geula C. Cholinergic innervation of the human striatum, globus pallidus, subthalamic nucleus, substantia nigra, and red nucleus. J Comp Neurol 1992;323:252–268. [PubMed: 1401259]
39. Bauer EP, Paz R, Pare D. Gamma oscillations coordinate amygdalo-rhinal interactions during learning. J Neurosci 2007;27:9369–9379. [PubMed: 17728450]
40. Paz R, Bauer EP, Pare D. Learning-related facilitation of rhinal interactions by medial prefrontal inputs. J Neurosci 2007;27:6542–6551. [PubMed: 17567815]
41. Paz R, Pelletier JG, Bauer EP, Pare D. Emotional enhancement of memory via amygdala-driven facilitation of rhinal interactions. Nat Neurosci 2006;9:1321–1329. [PubMed: 16964249]

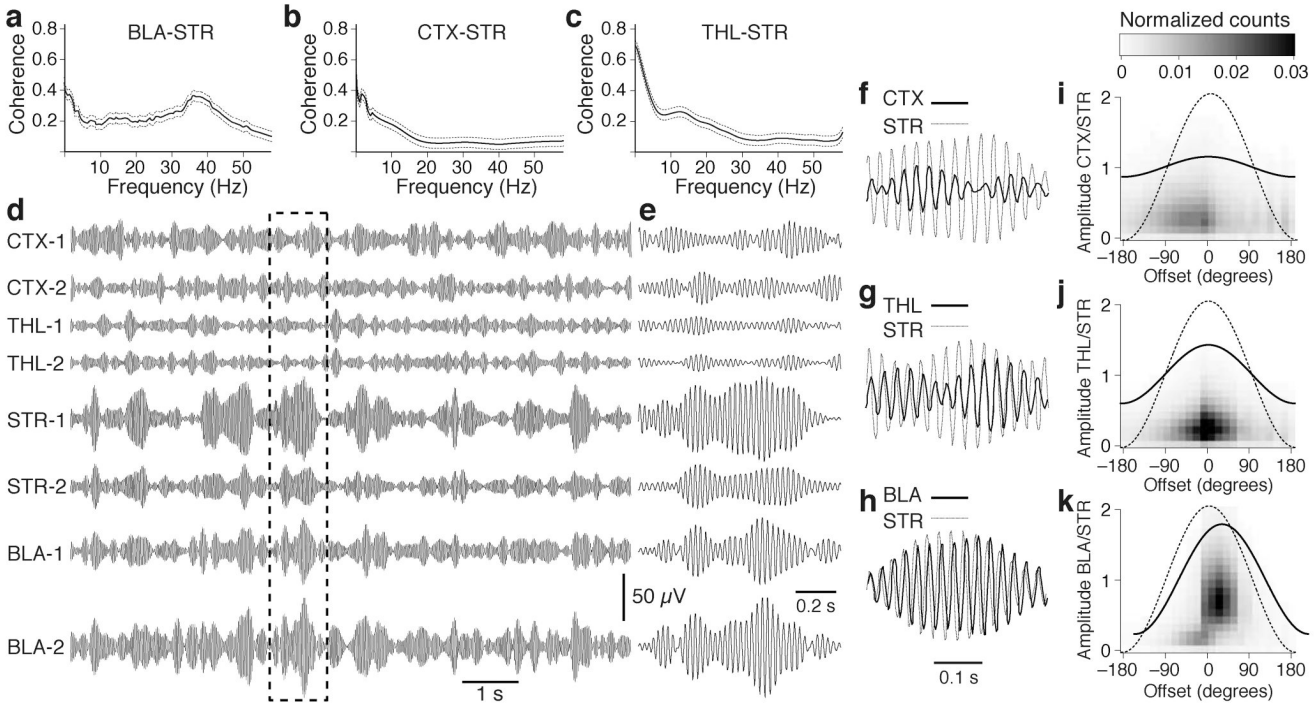

Fig. 1.

Coherent gamma activity in the BLA and ventral striatum during wakefulness. The graphs in **a–c** plot coherence ± s.e.m. (y-axis) vs. frequency (x-axis) for all available pairs of simultaneous LFP recordings in the BLA and striatum (STR; **a**; n = 696), auditory cortex (CTX) and striatum (**b**; n = 572) as well as intralaminar thalamus (THL; n = 304) and striatum (**c**). (**d, e**) LFPs simultaneously recorded at sites listed above and digitally filtered to isolate gamma (35–45 Hz) at a slow (**d**) and fast (**e**) time base. Dashed rectangle in **d** marks segment expanded in **e**. Panels **f–h** show brief period of high amplitude striatal gamma (thin line) superimposed with cortical (**f**), thalamic (**g**) and BLA (**h**) gamma (thick lines). Panels **i–k** plot normalized frequency distributions of phase lags (x-axis) between striatal vs. cortical (**i**), thalamic (**j**), or BLA (**k**) gamma as a function of normalized gamma amplitude (left y-axis). The lines overlaid on these graphs represent the average gamma cycles seen at the corresponding sites.

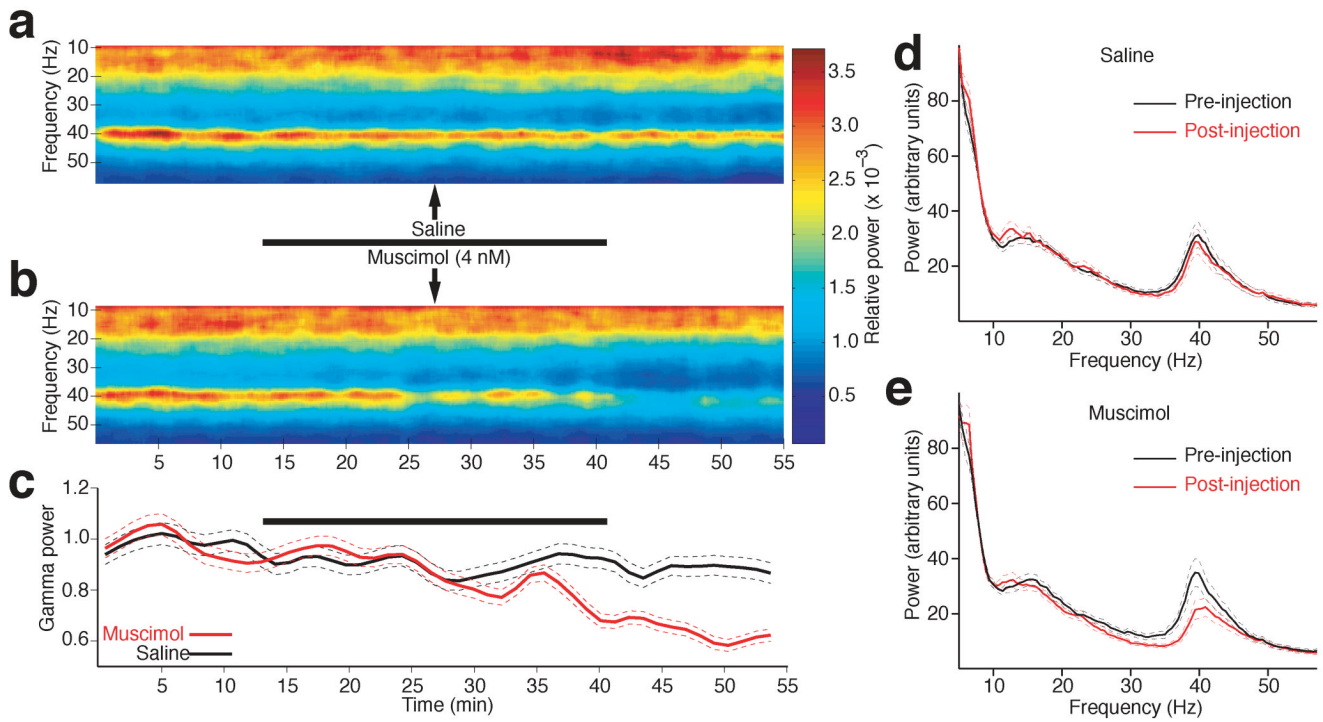

Fig. 2.

Intra-BLA muscimol infusions reduce striatal gamma power. (**a–b**) Striatal LFP power (color-coded) in different frequencies (y-axis) plotted as a function of time (x-axis) in experiments where either saline (**a**) or musci0mol (**b**) was slowly infused in the BLA, over a period of 25 min. (**c**) Gamma power (y-axis) ± s.e.m. (dashed lines) as a function of time (x-axis) when either saline (black) or muscimol (red) was infused in the BLA. In **a–c**, the thick black lines indicate infusion periods. (**d–e**) Power spectrum of striatal LFPs during the control (black) and post-infusion (red) phases in experiments where either saline (**d**) or muscimol (**e**) was infused in the BLA. Dashed lines indicate s.e.m.

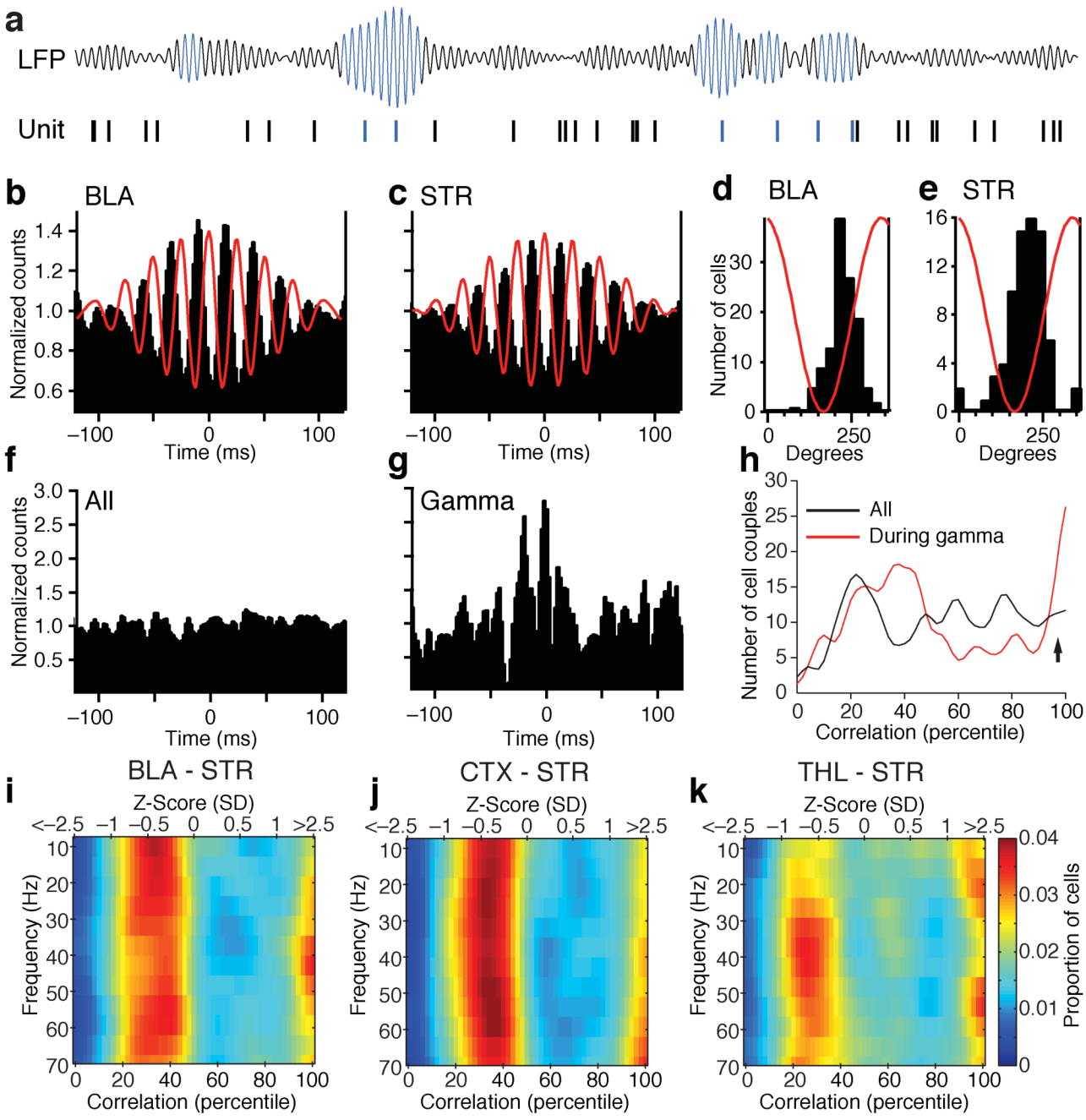

Fig. 3.

Gamma oscillations increase coupling between the activity of BLA and striatal neurons. (**a**) High amplitude gamma cycles were detected in the digitally filtered LFPs. Then, PEHs of unit activity were constructed around them. (**b–c**) Example of PEHs of BLA (**b**) and striatal (**c**) unit activity around the positive peaks of high amplitude gamma cycles. To facilitate comparisons between PEHs, we normalized the data in the following manner: the average bin value was computed and the bin values were divided by this average. (**d–e**) Frequency distributions of firing peak times for BLA (**d**) and striatal (**e**) neurons in relation to gamma. (**f**) Example of crosscorrelogram that included all spikes generated by a simultaneously recorded couple of BLA and striatal neurons. (**g**) Crosscorrelogram of unit activity for the same cell couple after

excluding striatal spikes occurring during periods of low amplitude gamma. (**h**) Percentiled frequency distribution of correlation indices in the crosscorrelograms of all BLA-striatal cell couples. Black, all spikes; Red, analysis restricted to striatal spikes occurring during high amplitude striatal gamma. (**i–k**) Color-coded frequency distributions of correlation indices (x-axis) plotted as a function of the frequency of striatal LFPs (y-axis) used to select spikes included in the crosscorrelograms. The bottom x-axis expresses the data in percentiles. The correspondence in Z-scores can be found in the top x-axis. This was done for all simultaneously recorded couples of BLA and striatal (**i**), cortical and striatal (**j**), or thalamic and striatal (**k**) neurons.

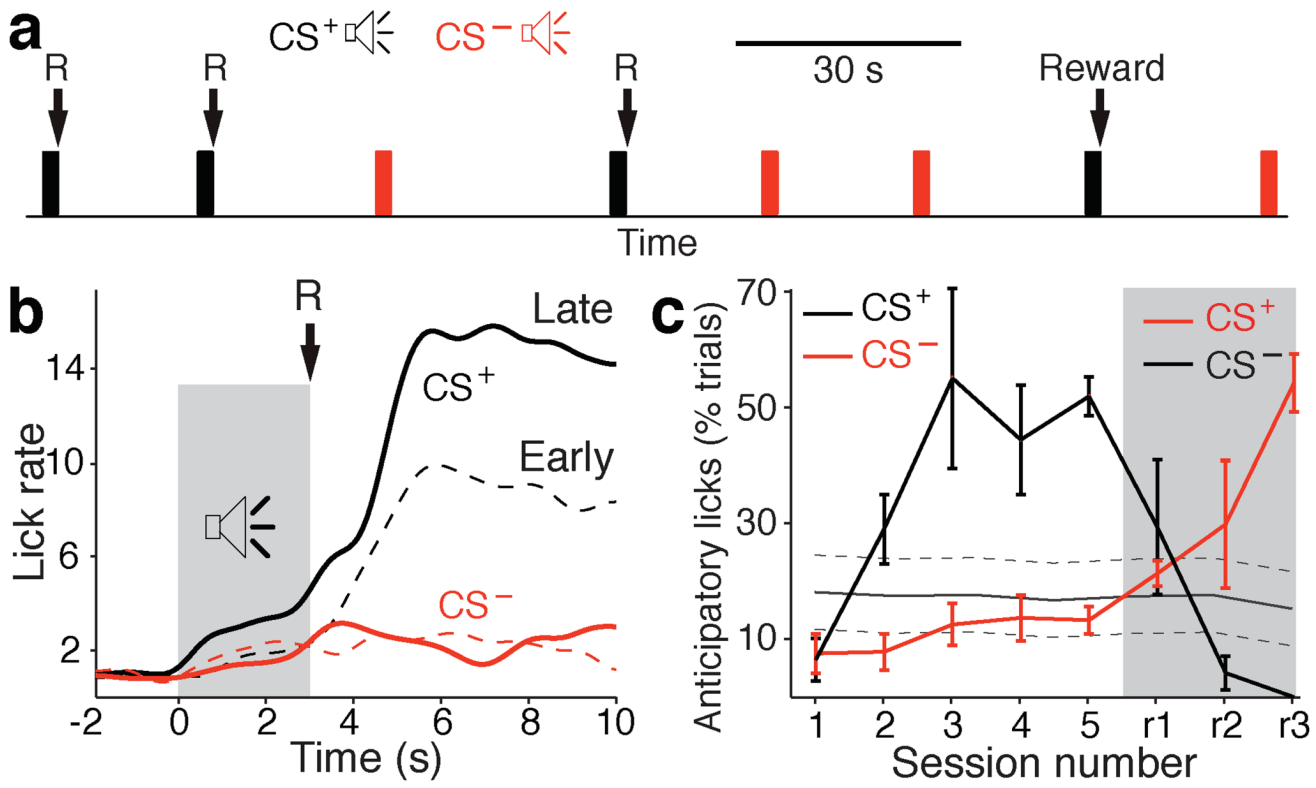

Fig. 4.

Progression of licking behavior during training on the stimulus-response task. (**a**) The animals were presented with two tones, one CS– (red) and one CS+ (black), in random order and with variable inter-tone intervals (20–40 s). The termination of the CS+ coincided with the delivery of a liquid reward (R). (**b**) Normalized licking frequency (y-axis) plotted as a function of time (x-axis) around the tone presentations (gray shading) at early (dashed line) and late (solid line) stages of learning (CS+, black; CS–, red). (**c**) Percent trials with anticipatory licks (y-axis) during the CS+ (black) and CS– (red) plotted as a function of daily training sessions (x-axis; sessions 1–5). Starting from session r1 (gray shaded area), the tone-reward contingencies were reversed. Gray line indicates proportion of trials with spontaneous licking ± s.e.m.

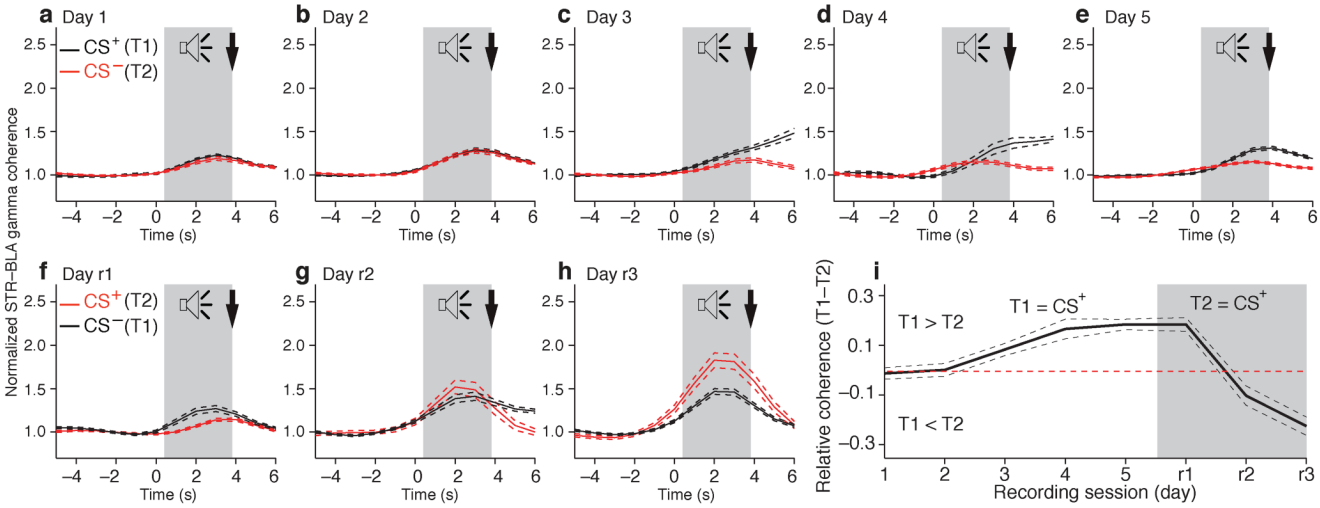

Fig. 5.

Learning-related changes in correlated amygdalo-striatal gamma. Striatal and BLA gamma power was calculated in one-second windows around tone onset. Striatal-BLA gamma coherence was estimated by computing the product of the BLA and striatal gamma power individually for each one second time window. (**a–h**), Coherence (y-axis) vs. time (x-axis) around onset of CS+ (black lines) and CS– (red lines) ± s.e.m. (dashed lines). Two tone-reward contingences were used: the first between training Days 1–5 (**a–e**) and the second, where the identities of the CS+ and CS– were reversed, between Days r1-r3 (**f–h**). (**i**) Difference in gamma coherence between the two tones (y-axis) as a function of recording sessions (x-axis).

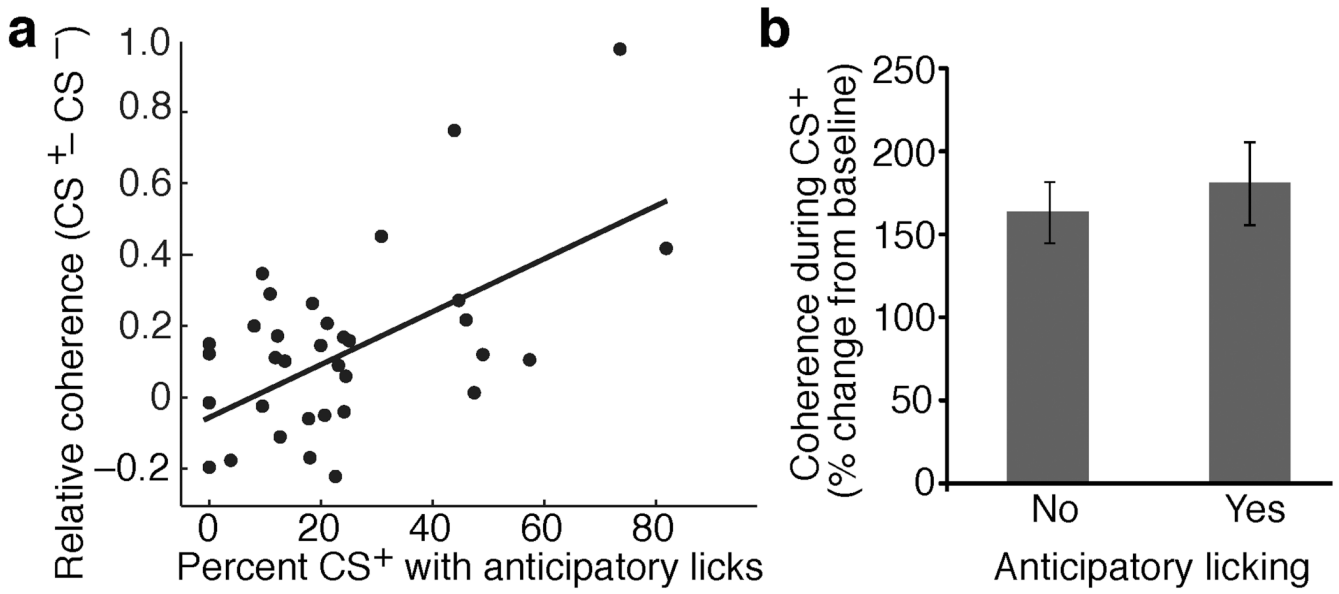

Fig. 6.

CS+ evoked increases in coherent BLA-striatal gamma parallel behavioral performance but are not caused by motor outputs. (**a**) Relationship between coherence of BLA-striatal gamma (y-axis) and proportion of CS+ trials with anticipatory licking (x-axis). Coherence values are relative ($CS^+ – CS^–$). Each data point represents a training session. A significant correlation was found ($r = 0.55$, $P < 0.01$). The correlation remains significant ($r = 0.37$, $P < 0.05$) even when the two top-most data points are excluded from the analysis. (**b**) Percent change in BLA-striatal gamma coherence during trials without (left) of with (right) anticipatory licking during the CS+. The difference is not significant (*t*-test, $P = 0.58$).